Available online at www.sciencedirect.com
SCIENCE DIRECT®
Optics Communications 247 (2005) 257–264
OPTICS COMMUNICATIONS
www.elsevier.com/locate/optcom

# New insights into the problem of shadowlike projection of a plane object illuminated by a spherical wavefront

José Azaña [a,*], J.E. Lugo [b], Andrew G. Kirk [b], David V. Plant [b]

[a] *Institut National de la Recherche Scientifique – Énergie, Matériaux et Télécommunication, 800 De la Gauchetière Ouest, Suite 6900, Montréal, Que., Canada H5A 1K6*
[b] *Department of Electrical and Computer Engineering, McGill University, Montréal Que., Canada H3A 2A7*

Received 5 June 2004; received in revised form 16 November 2004; accepted 17 November 2004

**Abstract**

The problem of diffraction from a plane object illuminated by a monochromatic point spherical wavefront is investigated using a Fourier-domain approach based on general diffraction theory. In particular, we focus on the so-called shadowlike projection phenomenon, i.e., when the diffraction patterns of the illuminated object are magnified or reduced images of the object. The analysis conducted here allows us to provide a general mathematical formulation of the shadowlike projection phenomenon, including a formal derivation of the known equations governing this phenomenon. More importantly, our analysis also offers a deeper insight into this phenomenon. As an example, it has been shown that under certain conditions, the spherical wavefront illumination can induce a space-to-angular spectrum conversion in the diffracted field. Here we report an experimental observation of this so-called angular Fraunhofer effect.


*PACS:* 42.25.F; 42.30
*Keywords:* Optical diffraction; Fourier optics

## 1. Introduction

The subject of diffraction from planar objects is treated in many textbooks; although the case of plane wavefront (parallel) illumination is more frequently considered, interesting diffraction phenomena related with the use of non-parallel illumination have also been described [1]. For instance, several authors have demonstrated that different focused laser beams (including diffracted converging spherical waves) can experience, under some specific circumstances, an unexpected focal shift effect, i.e., the point of maximum intensity of the beam along its propagation direction does not coincide with the geometrical focus [2–4].

* Corresoponding author. Tel.: +1 514 875 1266x3019; fax: +1 514 875 0344.
*E-mail addresses:* azana@inrs-emt.uquebec.ca (J. Azaña), plant@photonics.ece.mcgill.ca (D.V. Plant).

0030-4018/$ - see front matter 
doi:10.1016/j.optcom.2004.11.065

More in relation with our work, it has been recognized for a long time that a highly-magnified image of a given object can be projected onto a distant viewing screen by simply illuminating the object from an *appropriate* divergent light beam. This phenomenon, which we will refer to as shadowlike projection phenomenon, has been even evaluated as a potential alternative for electron microscopy of (sub)-micron specimens [5]. Similarly, one could also expect to obtain a reduced image of a given object by simply illuminating the object with an appropriate *convergent* light beam. The shadowlike projection phenomenon is usually described using a simplistic geometrical approach, and in fact, a simple interpretation of the phenomenon can be given in terms of a "generalized" Rayleigh range. Briefly, it is well-known that a pinhole illuminated by a plane wavefront produces an accurate "image" of the object (pinhole) up to the so-called Rayleigh distance [6]. Using a converging or diverging wavefront simply shifts this region and induces magnification in the generated image according to the lens law [7]. It should be also mentioned that the shadowlike projection phenomenon has an essentially different physical origin to that of the well-known lensless imaging phenomenon of a periodic plane object (Talbot effect) illuminated by a plane wavefront [8] or a spherical wavefront [9].

In this paper, we analyze the problem of shadowlike projection by point source illumination using a Fourier-domain approach based on general diffraction theory. This analysis allows us to obtain a general and complete mathematical formulation of the problem under analysis, thus providing a formal and elegant derivation of some of the known laws governing the shadowlike projection phenomenon (e.g., laws given by the geometric interpretation of the problem). Furthermore, our study also renders a much deeper insight into the physics of this phenomenon. Our preliminary studies in the subject [10] have already shown interesting, unknown features of the phenomenon, such as the fact that under some specific circumstances, the point source illumination (divergent spherical wavefront) will induce a space-to-angular spectrum conversion (where the angular spectrum of the propagating radiation is a replica of the object intensity distribution). This interesting effect was referred to as *angular Fraunhofer* and allowed us to offer an alternative explanation to the observation of magnified images of the original object within the far-field diffraction region (the analysis in [10] was in fact restricted to the far-field diffraction region). Here, we generalize this previous study and conduct a theoretical analysis which is valid for both the near-field and the far-field diffraction regions. Moreover, the analysis conducted here also considers both divergent and convergent illuminations. In this way, we provide a complete and solid physical explanation of the shadowlike projection phenomenon within the general diffraction-theory framework. As another important contribution of this present work, we have also conducted a series of experiments to confirm our main theoretical findings and for instance, we have observed the theoretically predicted space-to-angular spectrum conversion by point source illumination (angular Fraunhofer regime).

## 2. Theory

### 2.1. Diffraction analysis of the shadowlike projection phenomenon

Fig. 1 represents a schematic of the problem under analysis. We consider an arbitrary amplitude/

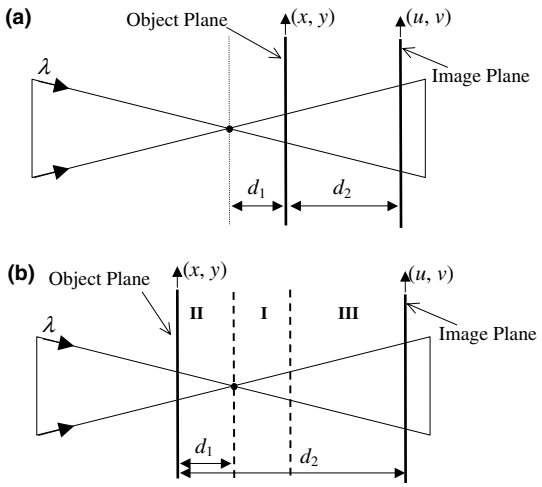


Fig. 1. Schematic of the problem under investigation: (a) divergent illumination; (b) convergent illumination.

phase plane object of complex amplitude transmission function $t(x, y)$, which is confined to an area of radius $\Delta r_1$, where $\Delta r_1^2 = \max(x^2 + y^2)$ for the transmission function of the object $t(x, y)$. The object is illuminated by a monochromatic *spherical wavefront* of wavelength $\lambda$. We consider two different cases, divergent and convergent illumination (see Fig. 1).

As shown in Fig. 1, the object is assumed to be located at a distance $d_1$ from the focus point of the spherical wavefront. Let us assume that this spherical wavefront can be approximated by a paraboloidal wavefront. This approximation is valid if the following condition is satisfied [1]

$$d_1 \gg \Delta r_1. \tag{1}$$

We will also assume that we work within the paraxial diffraction approximation. This approximation is valid if the angular spectrum of the field spatial distribution in the object plane is confined to an area of radius $\Delta k_{\text{field}}$, so that [1]

$$\Delta k_{\text{field}} \ll \frac{2\pi}{\lambda}. \tag{2}$$

Under the stated approximations, the field complex amplitude distribution $g(u, v)$ in a given transversal plane $(u, v)$, which is located at a distance $d_2$ from the illuminated object can be calculated using the Fresnel–Kirchoff integral as [1]

$$g(u,v) = g_0 \int_{-\infty}^{+\infty}\int_{-\infty}^{+\infty} f_{d_1}(x,y) \times \exp\left(-\mathrm{j}\frac{\pi}{\lambda d_2}\left[(u-x)^2 + (v-y)^2\right]\right)\mathrm{d}x\mathrm{d}y, \tag{3a}$$

$$f_{d_1}(x,y) = t(x,y)\exp\left(\mp\mathrm{j}\frac{\pi}{\lambda d_1}\left[x^2 + y^2\right]\right), \tag{3b}$$

where $g_0$ is a complex constant and $f_{d_1}(x,y)$ is the field complex amplitude distribution at the object plane (i.e., the transmission function of the object $t(x, y)$ multiplied by a quadratic phase function which is associated with the spherical wavefront illumination). In all our equations, the upper sign always holds for the case of divergent illumination (Fig. 1(a)) whereas the bottom sign always holds for the case of convergent illumination (Fig. 1(b)). At this point we note that the spherical wavefront only affects the phase of the field complex amplitude distribution (see Eq. (3b)). As a result, the spatial field intensity distribution in the object plane is fixed by the intensity transmission function of the object, $|f_{d_1}(x,y)|^2 \propto |t(x,y)|^2$, where the symbol $\propto$ indicates proportionality. However, the phase transformation introduced by the spherical wavefront modifies the original energy distribution in the spectral domain. In other words, the angular spectrum of the field distribution in the object plane, $\tilde{f}_{d_1}(k_x,k_y) = \Im\{f_{d_1}(x,y)\}$, differs from the angular spectrum of the object's transmission function, $\tilde{t}(k_x,k_y) = \Im\{t(x,y)\}$ (the symbol $\Im$ represents Fourier transform). By manipulating Eq. (3) we derive that

$$\begin{aligned} g(u,v) &= g_0\exp\left(-\mathrm{j}\frac{\pi}{\lambda d_2}\left[u^2+v^2\right]\right)\int_{-\infty}^{+\infty}\int_{-\infty}^{+\infty} f_D(x,y) \\ &\quad\times\exp\left(\mathrm{j}\frac{2\pi}{\lambda d_2}[ux+vy]\right)\mathrm{d}x\mathrm{d}y \\ &= g_0\exp\left(-\mathrm{j}\frac{\pi}{\lambda d_2}\left[u^2+v^2\right]\right) \\ &\quad\times\tilde{f}_D\left(k_x=-\frac{2\pi}{\lambda d_2}u, k_y=-\frac{2\pi}{\lambda d_2}v\right), \end{aligned} \tag{4a}$$

$$\frac{1}{D} = \frac{1}{d_2} \pm \frac{1}{d_1}, \tag{4b}$$

where $f_D(x, y) = t(x, y)\exp(-\mathrm{j}\pi[x^2 + y^2]/[\lambda D])$ and $\tilde{f}_D(k_x,k_y) = \Im\{f_D(x,y)\}$. The last integral has been solved by considering $\exp(\mathrm{j}(2\pi/\lambda d_2)[ux + vy])$ as the *kernel* of a Fourier integral. We note that for the Fourier transformations, we use the definition given by Papoulis in (Ref. [11] p. 1). The function $\tilde{f}_D(k_x,k_y)$ can be computed from its expression in the spatial domain $f_D(x, y)$ using well-known properties of the Fourier integral [11]

$$\tilde{f}_D(k_x,k_y) = \tilde{t}(k_x,k_y) \otimes A\exp\left(\mathrm{j}\frac{\lambda D}{4\pi}\left[k_x^2 + k_y^2\right]\right), \tag{5}$$

where the symbol $\otimes$ denotes convolution and $A$ is a complex constant. Eq. (5) results in a Fresnel–Kirchoff integral and consequently, under the conditions corresponding to the "far-field" (or Fraunhofer) approximation, Eq. (5) can be approximated by

$$\tilde{f}_D(k_x,k_y) \approx A \exp\left(\mathrm{j}\frac{\lambda D}{4\pi}\left[k_x^2+k_y^2\right]\right) \times t\left(x=-\frac{\lambda D}{2\pi}k_x, y=-\frac{\lambda D}{2\pi}k_y\right). \quad (6)$$

As the Fraunhofer formulation in the problem of spatial diffraction, the result in Eq. (6) can be obtained using the stationary-phase method (e.g., Appendix III in [1]). Nonetheless, for our purposes it is more convenient to use a Fourier-based approach for deriving Eq. (6). This approach allows us to estimate the condition under which the result in Eq. (6) is valid. This condition can be formulated as follows:

$$\lambda \mid D \mid \ll \frac{4\pi^2}{\Delta k_1^2}, \quad (7)$$

where $\Delta k_1$ is the spectral confinement radius of the object's transmission function, i.e., $\Delta k_1^2 = \max\left(k_x^2+k_y^2\right)$ for the angular spectrum function $\tilde{t}(k_x,k_y)$. We finally introduce Eq. (6) into Eq. (4) and obtain that

$$g(u,v) = B \exp\left(-\mathrm{j}\frac{\pi}{\lambda[d_2 \pm d_1]}\left[u^2+v^2\right]\right) \times t\left(x=\frac{1}{M}u, y=\frac{1}{M}v\right), \quad (8)$$

where $B = g_0 A$ is a constant and $M$ is the image magnification factor

$$M = 1 \pm \frac{d_2}{d_1}. \quad (9)$$

Eq. (8) indicates that, under the stated conditions, the intensity diffraction pattern $|g(u, v)|^2$ in the transversal plane $(u, v)$ is a replica (image) of the intensity distribution in the object plane, $|t(x, y)|^2$, the image magnification factor being given by Eq. (9). We recall that in the theoretical analysis conducted above no assumptions regarding the location of the image plane have been made, i.e., this analysis is valid for both near-field and far-field diffraction regions. We also note that the form of magnification in Eq. (9) coincides with that directly inferred from a geometrical interpretation of the shadowlike projection phenomenon. As expected, the observed image can be a magnified or a reduced replica of the original object and in particular, for divergent illumination only direct, magnified images can be observed, whereas for convergent illumination, one can produce: (i) direct, reduced images (region II in Fig. 1(b)); (ii) reversed, reduced images (region I in Fig. 1(b)); or (iii) reversed, magnified images of the original object (region III in Fig. 1(b)). It is also worth mentioning that an *aberration-free* imaging process is ensured only if the paraxial conditions given by Eqs. (1) and (2) are satisfied. In other words, deviations with respect to these conditions will translate into aberrations in the observed image.

### 2.2. Physical interpretation of the shadowlike projection phenomenon

#### 2.2.1. General Rayleigh range

The essential condition that ensures shadowlike projection at a specific plane $(u, v)$, which is located at a distance $d_2$ from the object plane, is given by inequality (7). We show here that this condition can be interpreted simply as a generalized Rayleigh range.

In order to ensure that inequality (7) is satisfied, a previous estimation of the maximum spectral confinement radius, $\Delta k_1$ corresponding to the object's transmission function is required. In other words, condition (7) essentially depends on the minimum spatial feature of the object, $\Delta r_{\min} \approx 2\pi/\Delta k_1$ (i.e., spatial resolution) and in particular, this condition can be expressed as

$$\mid D \mid \ll \Delta r_{\min}^2/\lambda \quad (10)$$

with $D$ given by Eq. (4b). It is important to note that strictly speaking, Eqs. (7) and (10) are equivalent *only* for amplitude objects (where the object's angular bandwidth can be estimated as the inverse of the object's spatial resolution, as shown above). In the case of a general object of amplitude and phase, the relationship between angular bandwidth and spatial resolution is not so straightforward (in general, $\Delta r_{\min} > 2\pi/\Delta k_1$) and consequently, the equivalence between the two equations is not ensured. We reiterate that in general, Eq. (7) represents the condition that actually needs to be satisfied to ensure shadow-like projection of the illuminated object (for a general object

of amplitude and phase, Eq. (7) is more restrictive than Eq. (10)).

Physically, inequality (10) can be interpreted as a generalization of the Rayleigh range for an individual resolution element ($\Delta r_{\min}$). We remind the reader that the Rayleigh criterion is usually considered as the condition for geometrical optics to be valid in the problem of diffraction and can be formulated as follows [6]. The diffraction effect of a monochromatic beam of wavelength $\lambda$ in a given aperture confined to an area of radius $\Delta r_{\min}$ is negligible for distances $d_2$ from the object plane well within the corresponding Rayleigh range, i.e., $d_2 \ll \Delta r_{\min}^2/\lambda$ [6]. Condition (10) represents a generalized Rayleigh range since this condition ensures the validity of the geometrical optics description in the *general* problem of an object illuminated by a spherical wavefront, which includes the *specific* problem of illumination by a parallel plane wavefront (when the focus point of the spherical wavefront $d_1$ is located at infinity). Note that the *conventional* Rayleigh condition can be derived as a particular case of our general condition in Eq. (10) when illumination by a plane wavefront is considered (i.e., when $d_1 \to \infty$). In fact, the equation for the general Rayleigh range (condition (10)) is the same as that of the conventional Rayleigh range [6], except that the real distance $d_2$ in the conventional equation is substituted by the distance $D$ (given by Eq. 4) in the general equation, i.e., the corresponding lens law (associated to the spherical wavefront illumination) is applied [7].

### 2.2.2. Angular Fraunhofer regime

In the specific case of *divergent illumination*, it can be easily inferred that if the condition (7) is satisfied for a given distance $d_2$ then it is necessarily satisfied for shorter distances. Consequently, in order to achieve a shadowlike projection of the illuminated object in *all the planes along the light propagation direction* (including near-field and far-field diffraction regions) we only have to ensure that inequality (7) (or the equivalent inequality (10)) holds for $d_2 \to \infty$. Under this assumption, condition (7) can be re-written as

$$\lambda d_1 \ll 4\pi^2/\Delta k_1^2 \tag{11}$$

or in terms of the object spatial resolution,

$$\lambda d_1 \ll \Delta r_{\min}^2. \tag{12}$$

Inequality (11) is precisely the condition derived in [10] assuming operation within the far-field diffraction zone. This condition has been derived here as a particularization of our more general analysis of the shadowlike projection phenomenon. We demonstrated that if inequality (11) is satisfied, then the field energy angular spectrum in the transversal planes along the light propagation direction, $|\tilde{f}_{d_1}(k_x,k_y)|^2$, is a replica (*image*) of the object intensity spatial distribution $|t(x, y)|^2$ [10]. We referred to this phenomenon (space-to-angular spectrum conversion) as *angular* Fraunhofer. The existence of this phenomenon could be also theoretically inferred from the more general analysis conducted in this present paper (i.e., by suitably manipulating the above equations). Notice that the fact that the angular spectrum of the spatial field distribution in the object plane is a replica of the object itself is intrinsically compatible with the presented theory: as predicted, the far-field (Fraunhofer) diffraction pattern, which is always a replica of the angular spectrum of the field in the object plane, will be in this case a magnified replica of the original object. We emphasize that in the case of divergent wave illumination, the condition for shadow-like projection in the far-field region (spectral Fraunhofer condition in Eqs. (11) or (12)) necessarily implies shadow-like projection along the whole near-field region. The opposite is not true: shadow-like projection in a given plane within the near-field region (as determined by Eqs. (7) or (10)) does not necessarily mean that the image projection extends over the far-field region. This is absolutely consistent with the behavior expected from general diffraction theory.

Condition (12) can be re-written as $\Delta r_{\min}^2/\lambda d_1 \gg 1$. According to the results from the previous studies on diffraction of convergent spherical wavefronts [2–4], this last condition ensures that the point of maximum intensity along the light propagation direction coincides with the focus given by conventional geometrical optics (i.e., no significant focal shift is observed). This is consistent with the fact that as discussed above, condition (12) essentially ensures the validity of

the geometrical optics description in the problem under consideration.

### 2.3. Analysis of particular cases of practical interest

We distinguish two main cases of practical interest:

1. *High-magnification lensless imaging system* ($|M| \gg 1$). A high-magnification system can be interesting for microscopy applications. High-magnification can be achieved using either divergent or convergent illumination. The observation plane must be located at a distance $d_2$ so that $d_2 \gg d_1$. In this case, it can be easily demonstrated that the condition for imaging (in terms of the object spatial resolution) can be re-written again as in (12). In other words, operation within the angular Fraunhofer regime must be ensured.
2. *High−reduction lensless imaging system* ($|M| \ll 1$). As an application example, a high-reduction system could be interesting for micro-lithography applications. High-reduction can be achieved using convergent illumination. The observation plane must be located around the focus point of the spherical wavefront, i.e., $d_2 \to d_1$. Under these assumptions, it can be easily demonstrated that $|D| \approx d_1/|M|$ and the corresponding condition for lensless imaging (in terms of the object spatial resolution) can be re-written as

$$\lambda d_1 \ll | M | \Delta r_{\min}^2. \tag{13}$$

Note that both conditions (12) and (13) refer to the characteristic parameters of the illumination beam, namely the object-focus distance $d_1$ and the operation wavelength $\lambda$, and depend on the minimum spatial feature to be resolved $\Delta r_{\min}$. In general, the conditions for lensless imaging are more restrictive as the required spatial resolution decreases (i.e., the product $\lambda d_1$ must be smaller for smaller spatial resolutions). It is also worth noting that the condition for the case of image reduction (*inequality* (13), with $|M| \ll 1$) is much more restrictive than the condition for magnification (*inequality* (12)). In other words, entering the spectral Fraunhofer regime (space-to-angular spectrum conversion) does not necessarily ensure shadow-like projection imaging in the vicinity of the focus point of the convergent spherical wavefront (high-reduction lensless imaging).

## 3. Experimental observation of the angular Fraunhofer regime

We report the experimental observation of the predicted space-to-angular spectrum conversion by point source illumination (divergent illumination). Our experiments deal with the case of divergent illumination mainly due to practical reasons as this facilitates very much the observation of the obtained diffraction patterns (in the near-field region) while still providing the desired experimental evidence. The object used in our experiments was an irregular cross-like shape aperture, see inset in Fig. 2. This object was illuminated with a divergent spherical wavefront which was created by focusing the light from a HeNe laser ($\lambda \approx 632$ nm) onto a 50× microscope objective (numerical aperture of ≈0.42).

Fig. 2 shows the diffraction patterns of the object in both the near-field (Fresnel) and the far-field (Fraunhofer) diffraction zones. The patterns were captured with a conventional CCD camera. Specifically, in Fig. 2(a), the object was located at a distance $d_1 = 353$ mm from the point source, the near-field diffraction pattern was observed at a distance $d_2 = 457$ mm from the object and the far-field diffraction pattern was observed at the focal distance of an ordinary convex lens (focal length = 80 mm) placed right after the object. We emphasize that the proposed lens configuration allows us to measure the *angular spectrum of the spatial field distribution* at the object plane and not the spectrum of the object itself. We remind the reader that: (i) both spectra are different by virtue of the spherical wavefront illumination; (ii) the diffraction pattern observed in the far-field region coincides with the angular spectrum of the spatial field distribution (this was confirmed by direct observation of the far-field diffraction pattern in our problem; the use of the described Fourier setup in our experiments was necessary

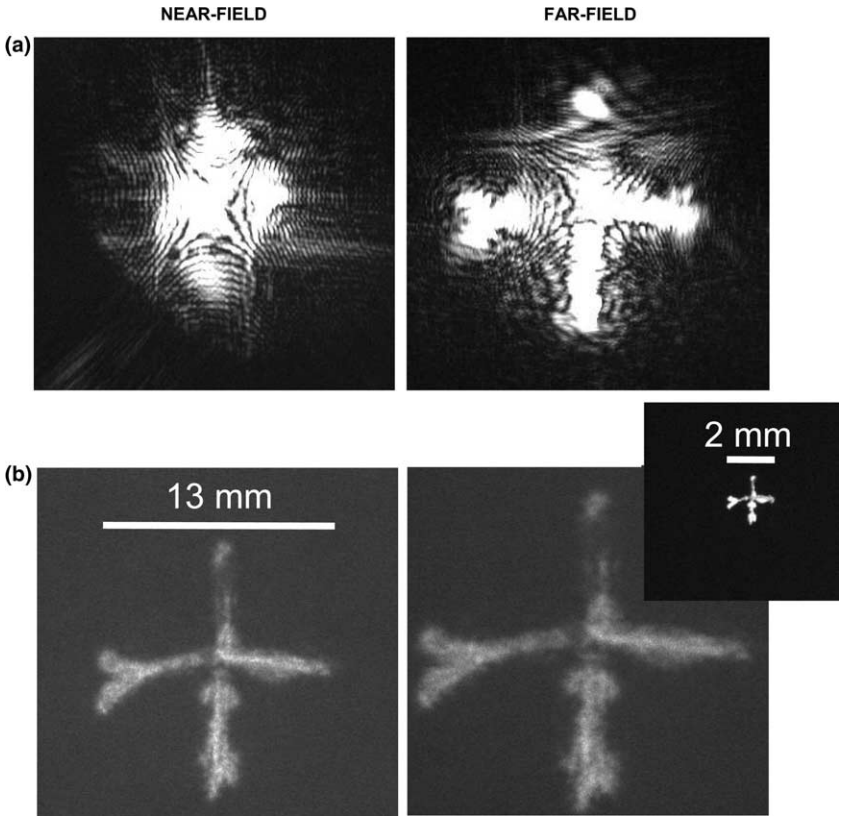


Fig. 2. Results from experiments: (a) near-field (Fresnel) and far-field (Fraunhofer) diffraction patterns when the object (cross-like aperture shown in the inset) is located at a distance $d_1 = 353$ mm from the point source (out of shadowlike projection regime); and (b) when the object is located at a distance $d_1 = 14.35$ mm from the point source (within angular Fraunhofer regime).

to facilitate the capture of the far-field diffraction pattern by our CCD camera). In this first experiment (Fig. 2(a)) the object was located at a distance $d_1$ long enough to ensure that the condition for shadowlike projection at the observation distances (inequality (7)) is not satisfied. As expected, conventional diffraction patterns were observed and no image of the object was obtained.

In contrast, in the case of Fig. 2(b), the object was located at a distance $d_1 = 14.35$ mm from the point source, which is short enough to fulfil inequality (11), thus ensuring operation within the angular Fraunhofer regime, i.e., according to our theoretical predictions, we should achieve shadowlike projection along all the light propagation direction (for $0 \leqslant d_2 \leqslant \infty$). In the specific plots shown herein, the near-field diffraction pattern was measured at a distance $d_2 = 80.82$ mm from the object and the far-field diffraction pattern (angular spectrum of the spatial field distribution) was measured using the same lens and procedure as before. As predicted by the theory, a magnified image of the original object was observed on all the transversal planes along the light propagation direction, within both the near-field and the far-field diffraction regions (the image magnification factor increasing with the observation plane-object distance, according to relation (9)). We point out the fact that the angular spectrum of the transversal spatial field distribution (far-field pattern) is also a replica (image) of the original object. In other words, the theoretically predicted space-to-angular spectrum conversion is observed.

## 4. Conclusions

Summarizing, in this letter the problem of shadowlike projection of a plane object illuminated by a monochromatic spherical wavefront has been explained within the context of general diffraction theory (Fourier – domain approach), thus providing a deeper insight into the physics of this problem. From this study, a general mathematical formulation of the shadowlike projection phenomenon has been derived (this includes an elegant derivation of the more conventional formulation of the problem) and some essential and interesting features of the phenomenon have been described. Our formulation of the problem is valid for a general plane object of amplitude and phase. From our general formulation of the problem, we have derived the required conditions to achieve a high-magnification lensless imaging process (e.g., of interest for microscopy applications) or a high-reduction lensless imaging process (e.g., of interest for micro-lithography applications). In all the cases, the required conditions refer to the parameters of the illumination source (product of wavelength by object-focus distance) and our equations show that these conditions are in fact much more restrictive for the case of image reduction than for the case of magnification. It has been also shown that in order to achieve a high-magnification imaging process (i.e., shadow-like projection in the far-field region), the spherical wavefront must induce a space-to-angular spectrum conversion in the propagating radiation. Finally, we have reported an experimental observation of this so-called angular Fraunhofer phenomenon.

## Acknowledgements

This research was supported in part by the Natural Sciences and Engineering Research Council (NSERC) and industrial and government partners, through the Agile All-Photonic Networks (AAPN) Research Network, by the Fonds Québécois de la Recherche sur la Nature et des Technologies (FQRNT), and by Nanoquebec.

## References

[1] M. Born, E. Wolf, Principles of Optics, sixth ed., Pergamon Press, London, 1989.
[2] E. Wolf, Y. Li, Opt. Commun. 39 (1981) 205.
[3] Y. Li, E. Wolf, Opt. Commun. 39 (1981) 211.
[4] W.H. Carter, Appl. Opt. 21 (1982) 1989.
[5] G.A. Morton, E.G. Ramberg, Phys. Rev. 56 (1939) 705.
[6] See for instance Section 4.2.2 of J.W. Goodman, Introduction to Fourier Optics, second ed., McGraw-Hill, New York, 1996.
[7] See for instance, J. Shamir, Optical Systems and Processes, SPIE Optical Engineering Press, Bellingham, Washington, 1999, Appendix A.
[8] K. Patorski, in: E. Wolf (Ed.), Progress in Optics XXVII, Elsevier Science, Amsterdam, The Netherlands, 1989, p. 1.
[9] J.M. Cowley, A.F. Moodie, Proc. Phys. Soc. 70 (1957) 486.
[10] J. Azaña, Opt. Lett. 28 (2003) 501.
[11] A. Papoulis, The Fourier Integral and its Applications, McGraw-Hill, New York, 1962.